Istraživanja i projektovanja za privredu
ISSN 1451-4117
DOI:10.5937/jaes0-40435
www.engineeringscience.rs

iipp publishing

Journal of Applied Engineering Science
Vol. 21, No. 1, 2023
Original Scientific Paper
Paper number: 21(2023)1, 1075, 326-335

ELECTROMECHANICAL PROPERTIES OF SELF-SENSING CEMENT PASTES POLARIZED WHILE FRESH

Mohammad Al-Qaralleh

Civil and Environmental Engineering Department, College of Engineering, Mutah University, Alkarak, Jordan.
Member of the Materials' Science and Energy Lab in Mutah University

** mohammad.alqaralleh@mutah.edu.jo*

This work investigates the bulk resistivity, and the stress-strain relationship of polarized cement paste as indicators of its electromechanical properties. The polarizing of the cement paste specimens was achieved by applying a uniform direct current (DC) electric field through the fresh cement paste for 24 hours. A total of 24 specimens were prepared for this study, 7 of them were not cured under the effect of the DC electric field to serve as reference. 3 different electrical field values were utilized in this experiment, namely: 100 V.m^{-1}, 200 V.m^{-1}, and 500 V.m^{-1}. 2 types of water were used for mixing the cement paste, namely: tap (T), and deionized (DI). The bulk resistivity values were measured in the direction parallel to the polarization, and the two other directions perpendicular to the polarization. The T water specimens were tested under uniaxial compression on the axis of polarization. The results show that the bulk resistivity of the specimens was increased as the curing electrical field increased. Mixing with T water also increased the bulk resistivity when compared to mixing with DI water. Polarizing the fresh cement paste has a significant effect on its mechanical properties such that the ultimate compressive strength decreased by 50%, and the failure strain increased by 500%. In addition, the polarized specimens showed some changes in its morphology when compared with the reference.

Keywords: polarizing, fresh cement paste, self-sensing, bulk resistivity, structural health monitoring (SHM)

1 INTRODUCTION

Structural Health Monitoring (SHM) is extremely important to avoid catastrophic events. This subject has been, and still is, of interest of the scientists and researchers. SHM can be achieved by monitoring the state of the stresses in the structural elements in real-time. Some structures even requires a permanent and automated monitoring systems to avoid any unexpected events that might jeopardize its integrity [1]. This can be essentially achieved by using either non-intrinsic sensors or intrinsic sensors [2–5]. If the stresses in the structural element is known, its life expectancy can be easily calculated using the simple beam theory [6]. The non-intrinsic sensors is based on utilizing external sensing devices such as: strain gauges, fiber optic sensors, and piezoelectric sensors [7]. While the intrinsic sensors are based on enhancing the self-sensing capabilities of the material. Sensors rely on electrical circuits to report the changes that occur to the position and/or the strain of the structural element [4]. Hence, all the parts of this electrical circuit should have precisely defined electrical properties, such as: conductivity, piezoresistivity, and capacitance. Since a significant number of the structures in the world are made of concrete, it was apparent for the researchers that integrating the concrete into the sensing circuits will be highly beneficial. An early work by Whittington et al. [8] introduced a theoretical model to describe the mechanism of the electrical conduction in the concrete. Among the first attempts to investigate the idea of self-sensing concrete is the work of Chen & Chung [9], which yielded on promising results and paved the way for further enhancements. Many researchers tried to enhance the electrical properties of the concrete to achieve the mentioned goal by utilizing different functional fillers, such as: steel fibers, carbon fibers, nickel powder, graphite powder, glass powder, carbon nanotubes (CNT), steel slag, and silica fume [10–14]. Good reviews about such studies can be found in the literature [4,15–19]. However, utilizing the conductive fillers often faces the obstacle of the uniform distribution, which hinders its use for large scale structures [18]. Hence, it is obvious that the benefits of enhancing the sensing capabilities of the concrete without any additives will be more effective and economical. Previously, researchers tried to utilize the capacitance measurements as a sensing technique of the cement pastes without any added materials [20].

Polarization occurs in dielectric materials when an electrical field is applied on it, and in the case of cement paste, the present of moisture is essential for polarization to enhance the ionic conductivity [21]. Applying an electrical field on the cement paste liberates the dipoles to take the orientation of the field and form a chain of dipoles between the electrodes [22,23]. The polarizing effect of a Direct Current (DC) passing through cement hydrates was observed and reported in the literature. As mentioned before, electricity is essential in SHM, and it was utilized for Non-Destructive Testing (NDT) of concrete. However, the DC was avoided due to its polarization effect on the concrete in some tests such as the bulk resistivity test [24]. In addition, passing DC in concrete specimens, drives the ions in the direction of the electric field according to the so-called "electromigration" phenomenon [25]. Electromigration proved to be very beneficial for accelerating the Chloride ions permeability test [26], which is an important indicator of the status of the strength and integrity of the concrete. However, electromigration induces electrokinetic forces called the electro-osmosis that is responsible of increased stresses and shape modifications in the pore structure of the cement paste [25,27]. While the hardened cement pastes can be polarized, the polarization tends to be temporary

and reversible [23]. The effect of polarizing of hardened cement pastes on its electrical properties will vanish after disconnecting the polarizing current.

Polarization can be achieved by applying a uniform electrical field on the fresh cement paste specimen while curing [28,29]. This technique has multiple advantages when compared to the others mentioned before. In addition, it showed good results in enhancing the piezoelectric properties of the cement paste [29]. The DC curing of fresh cement paste improves its intrinsic piezoelectric properties without the need of adding functional fillers. In addition, once the cement paste hardens, the ions are arrested in the polarized position, which prevents the depolarizing phenomenon [23]. However, this technique still needs more investigation to fully understand the behavior of the cement hydrates products. The author previously investigated the effect of w/c on the piezoelectric properties of the treated specimens [30]. The results showed that changing the w/c ratio had negligible effect on the piezoelectric behavior of the tested specimens. Another study by the author [28] tested the relationship between the amplitude of the applied load on the treated specimens and their piezoelectric response. The results showed that the specimens produced a piezoelectric voltage that is directly related to the amplitude of the loading when tested parallel to the polarizing axis. This observation indicates that the piezoelectric response of the treated specimens can be utilized in self-sensing applications. A recent study by the author [29] further investigated the piezoelectric behavior of freshly polarized specimens. The study reported the effect of using different values of the DC potential, the effect of the different types of mixing water, and the moisture content on the overall piezoelectric behavior, as well as, the bulk density of the hardened cement paste.

1.1 Research significance

Utilizing the DC electrical field to polarize cement pastes while fresh has been previously presented by the author [28–30]. This polarization can enhance the intrinsic self-sensing properties of the cement pastes. However, this innovative technique still needs more investigation. This study aims at investigating the effect of the described polarizing technique on the electromechanical properties of the resulted hardened cement paste. To achieve that, the author investigated the bulk resistivity and the stress-strain relationships of the specimens. In addition, the effect of the type of mixing water on the bulk resistivity was reported.

2 METHODS

For this work, a total of 24 (50 × 50 × 50 mm) cement paste cubes were prepared according to the ASTM C109 [31]. 12 specimens were mixed with deionized (DI) water and other 12 were mixed with tap (T) water. 3 specimens of the T mix and 4 specimens of the DI mix were cast in standard brass molds to serve as reference. The rest of the specimens were cast in insulated plastic molds, and were cured for 24 hours while a DC passes through two opposite sides of each cube using stainless steel plates as electrodes as shown in Figure 1. The DC induced a uniform electric field on the cured specimens equals to the voltage divided by the distance between the two electrodes. The T specimens were cured in 3 patches under different electric field values, while the DI specimens were cured in 2 patches under different electric field values. The chosen electric field values were: 100 $V.m^{-1}$, 200 $V.m^{-1}$, and 500 $V.m^{-1}$. The notations of the specimens include the type of mixing water, the electric field value, and a number represents the proximity of the specimen to the power supply, for example: the specimen T100-2 was mixed with T water, cured under the effect of electric field equals to 100 $V.m^{-1}$, and is the second specimen in the patch. The reference specimens were given a 000 in the location of the electric field, for example: DI000-3, the notations of all the specimens are shown in Table 1. More information about the experimental methods and properties of the materials can be found in a previous article by the author [29].

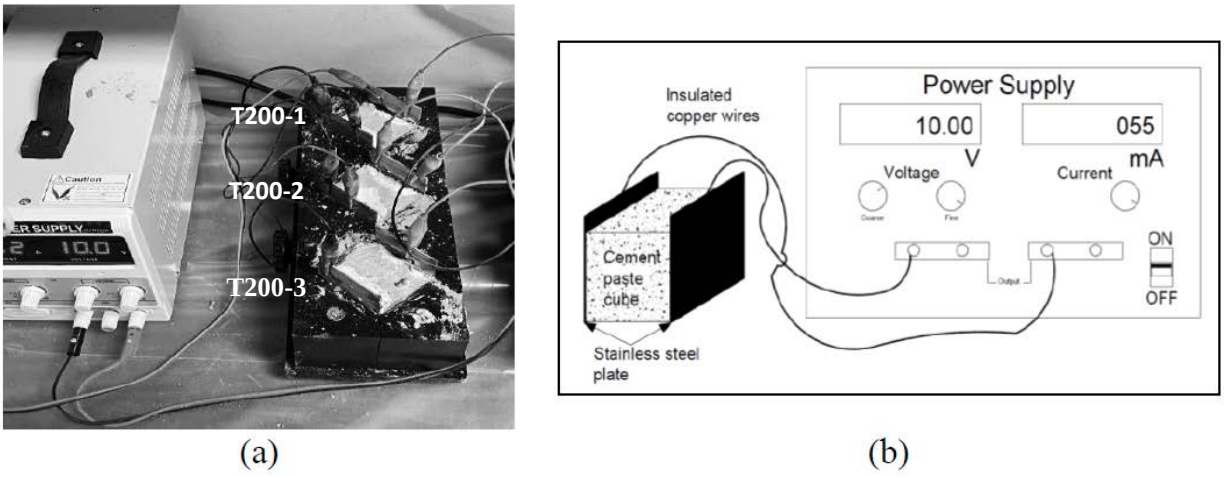

Figure 1: (a) Curing of the specimens while applying the DC current, (b) Schematic of the curing setup

After 24 hours from casting the specimens, they were all demolded, and all of their faces were sanded to remove any irregularities to ensure good contact with the electrodes for the bulk resistivity test. The dimensions of each

specimen were measured and recorded to be utilized in the bulk resistivity calculations later. In addition, the faces that were touching the electrodes in the polarized specimens were marked to test the electrical resistivity in the direction of polarization. Any excess moisture on the surfaces of the specimens was wiped off by a clean absorbent cloth. After demolding, the first measurement of the electrical resistivity was recorded for all the specimens, then the specimens were placed in a curing water path for 7 days. Then another run to measure the electrical resistivity values was performed.

2.1 Bulk resistivity test

The Resipod Proceq concrete resistivity meter with the bulk resistivity accessories was employed to measure the bulk resistivity of all the specimens (Figure 2). The device is originally designed as a Wenner probe, however, with the plates provided by the manufacturer, it can be used for measuring the bulk resistivity (ρ_{BR}) according to the following procedure:

The device measures the total surface resistivity (ρ_{SRT}) between the plates in kΩ.cm units, which incorporates a correction factor $k_1 = 2\pi a$, where a = the probe spacing which equals to 38 mm. The resistance of the moist foam inserts (R_F) that were utilized to ensure good contact between the plates and the surfaces of the specimen should be subtracted from the ρ_{SRT}. Hence, the true surface resistivity of the specimen $\rho_{SR} = \rho_{SRT} - R_F$. Then:

$$\rho_{SR} = k_1 * R \tag{1}$$

where R is the resistance. If A: is the cross-sectional area of the specimen and L: is the distance between the two electrodes (i.e. the length of the specimen), the ρ_{BR} can be written in the following formula:

$$\rho_{BR} = R * (A/L) \tag{2}$$

Solving equations 1, and 2, will result in equation 3 for calculating the ρ_{BR} directly from the reading of the Resipod Proceq device (ρ_{SR}), as following:

$$\rho_{BR} = \frac{\rho_{SR}}{k_1} * (A/L) \tag{3}$$

for the specific device that were used in this work, the factor is k_1 = 23.88 cm.

Figure 2: Resipod Proceq concrete resistivity meter

If the corner of the specimen is placed on the origin of the Cartesian coordinates, the polarization field was applied on the x-direction, and the top and bottom faces of the specimen were on the y-direction. When the $\rho_{SR}$was measured on a direction parallel to the polarization field it was recorded as ρ_{SRxx}. The ρ_{SRxy}, and ρ_{SRxz} correspond to the surface resistivities that were measured on perpendicular directions to the polarization field on the y-direction and z-direction, respectively. The measurements of the ρ_{SR} were implemented and recorded for all opposite surfaces of all the specimens as shown in Figure 3.

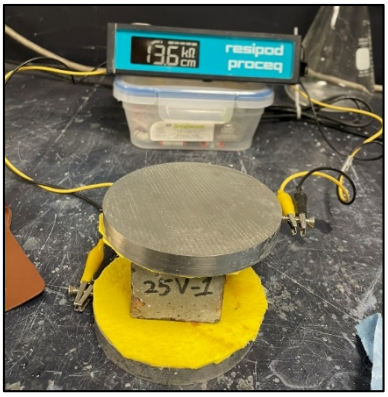

Figure 3: Bulk resistivity setup for one of the specimens

2.2 Compression test

The reference specimens and 2 specimens of each treated patch from the T water group were tested under compression to study the effect of the polarization on the mechanical properties of the hardened cement pastes. The rest of the specimens from the T water group, as well as, the specimens from the DI water group were spared for further testing. The compressive force was applied parallel to the polarization axis. The top and bottom faces of the reference specimens were avoided in the compression testing. To eliminate the effect of the stress gradient of the specimens, 2 neoprene pads were cut to size (50 × 50 mm) and placed between the testing machine and the faces of the specimens. The age of the specimens when the compression test was implemented was approximately 1 year.

3 RESULTS AND DISCUSSION

The ρ_{SR} of the specimens on all opposite faces was measured and recorded according to the procedure described before. The measurements were implemented twice, namely: directly after the demolding of the specimens, and after removing the specimens from the curing water path. The resistance of the upper and the lower moist foam inserts (R_F) each measured 1.4 kΩ.cm. The ρ_{BR} was then calculated according to Eq. (3), and all the values are listed in Table 1.

Table 1: Calculated Values of the ρ_{BR} for all the specimens

Specimen	(At demolding) ρ_{BR} [kΩ.cm]			(After curing) ρ_{BR} [kΩ.cm]		
	$\boldsymbol{\rho_{BRxx}}$	$\boldsymbol{\rho_{BRxy}}$	$\boldsymbol{\rho_{BRxz}}$	$\boldsymbol{\rho_{BRxx}}$	$\boldsymbol{\rho_{BRxy}}$	$\boldsymbol{\rho_{BRxz}}$
T000-1	0.743	1.009	0.749	2.378	2.944	2.268
T000-2	0.811	0.930	0.732	2.477	2.751	2.346
T000-3	0.788	0.879	0.754	2.491	2.722	2.282
μ	**0.781**	**0.940**	**0.745**	**2.449**	**2.805**	**2.299**
σ	**0.034**	**0.065**	**0.012**	**0.061**	**0.120**	**0.042**
T100-1	1.449	1.567	1.344	2.581	2.511	2.458
T100-2	1.425	1.546	1.365	2.578	2.656	2.532
T100-3	1.356	1.505	1.292	2.528	2.521	2.467
μ	**1.410**	**1.539**	**1.334**	**2.562**	**2.563**	**2.485**
σ	**0.048**	**0.032**	**0.038**	**0.030**	**0.081**	**0.041**
T200-1	2.016	1.981	1.839	2.789	2.616	2.643
T200-2	2.001	2.007	1.707	2.617	2.595	2.532
T200-3	2.047	2.013	1.799	2.700	2.738	2.603
μ	**2.022**	**2.000**	**1.782**	**2.702**	**2.650**	**2.593**
σ	**0.024**	**0.017**	**0.067**	**0.086**	**0.077**	**0.056**
T500-1	3.493	2.585	2.346	3.516	3.369	3.431
T500-2	3.433	3.054	2.939	3.753	3.645	3.565
T500-3	3.370	3.627	2.723	3.529	4.006	3.389
μ	**3.432**	**3.089**	**2.670**	**3.599**	**3.673**	**3.462**
σ	**0.062**	**0.522**	**0.300**	**0.133**	**0.320**	**0.092**
DI000-1	0.985	1.002	1.001	1.781	2.004	1.788
DI000-2	0.989	0.980	0.995	1.768	1.940	1.737
DI000-3	1.027	1.011	0.985	1.782	2.064	1.739
DI000-4	1.054	1.024	1.008	1.829	2.111	1.764
μ	**1.014**	**1.004**	**0.997**	**1.790**	**2.030**	**1.757**
σ	**0.033**	**0.018**	**0.010**	**0.027**	**0.074**	**0.024**
DI200-1	1.782	1.611	1.615	2.014	2.063	2.048

Specimen	(At demolding) ρ_{BR} [kΩ.cm]			(After curing) ρ_{BR} [kΩ.cm]		
DI200-2	1.848	1.652	1.729	1.961	2.055	2.040
DI200-3	1.820	1.777	1.537	1.957	2.056	1.990
DI200-4	1.723	2.073	1.758	2.082	2.169	2.153
μ	**1.793**	**1.778**	**1.660**	**2.003**	**2.086**	**2.058**
σ	**0.054**	**0.209**	**0.103**	**0.059**	**0.055**	**0.069**
DI500-1	2.885	2.909	2.228	2.453	2.519	2.505
DI500-2	2.775	2.802	2.129	2.570	2.602	2.558
DI500-3	2.266	2.605	1.903	2.449	2.507	2.466
DI500-4	3.120	2.581	2.152	2.687	2.640	2.676
μ	**2.761**	**2.724**	**2.103**	**2.540**	**2.567**	**2.551**
σ	**0.360**	**0.158**	**0.140**	**0.113**	**0.064**	**0.091**

The mean (μ) and the standard deviation (σ) of the results listed in Table 1 was calculated for each patch of specimens and each direction of bulk resistivity measurement. The μ results were plotted with the σ values shown as error bars on top of each patch as shown in Figure 4, Figure 5, Figure 6, Figure 7, Figure 8, and Figure 9. The ρ_{BRxx} for all the patches at demolding and after water-bath curing are shown in Figure 4, and Figure 7, respectively. The ρ_{BRxy} for all the patches at demolding and after water-bath curing are shown in Figure 5, and Figure 8, respectively. Lastly, the ρ_{BRxz} for all the patches at demolding and after water-bath curing are shown in Figure 6, and Figure 9, respectively. The measured ρ_{BR} values of all the specimens show considerable consistency for the same patch and direction of measurement, which is apparent from the σ values in the figures mentioned. However, the specimens that were polarized by a 500 V.m^{-1} electric field show higher discrepancy in the measured ρ_{BR} values when compared to the other patches. In general, it is safe to say that the ρ_{BR} is more consistent when compared to the piezoelectricity measurement of the same specimens [29].

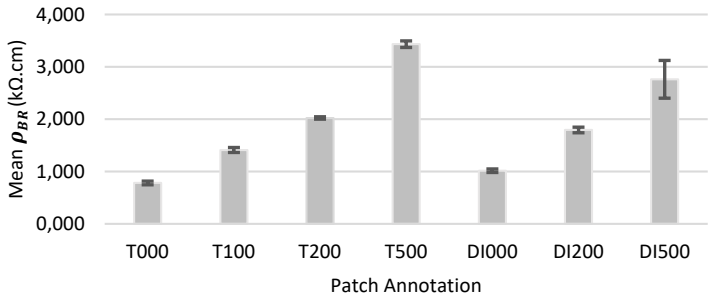

Figure 4: Mean values of ρ_{BRxx} for all the specimens at demolding

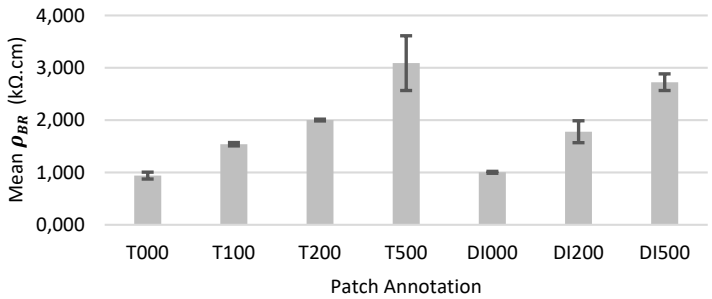

Figure 5: Mean values of ρ_{BRxy} for all the specimens at demolding

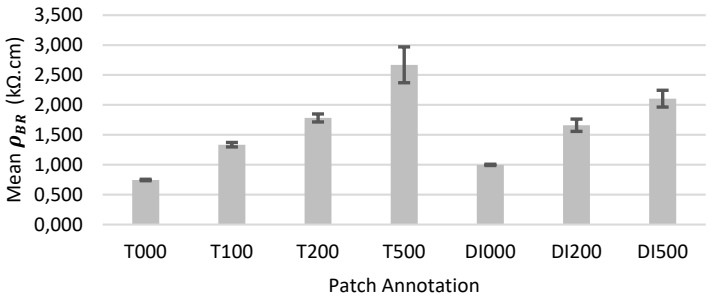

Figure 6: Mean values of ρ_{BRxz} for all the specimens at demolding

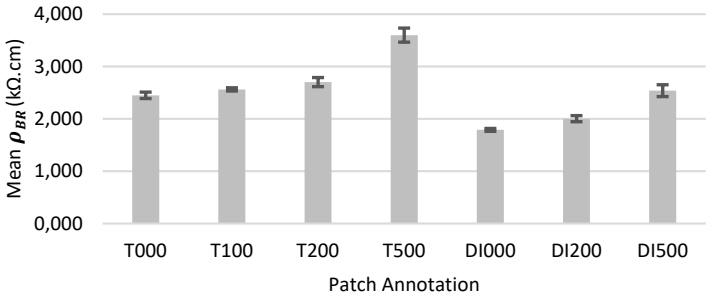

Figure 7: Mean values of ρ_{BRxx} for all the specimens after curing

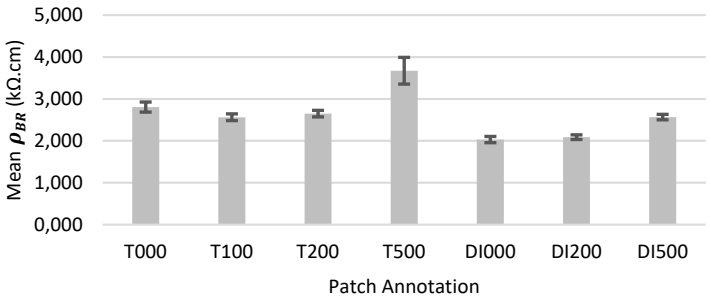

Figure 8: Mean values of ρ_{BRxy} for all the specimens after curing

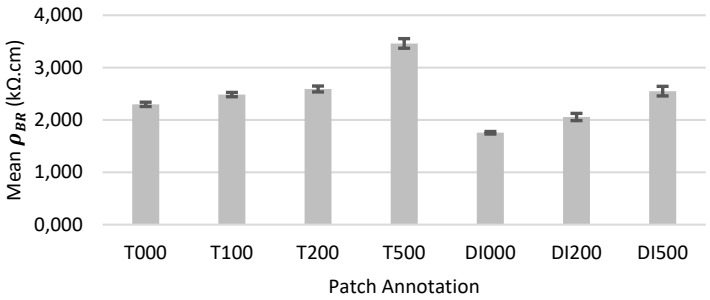

Figure 9: Mean values of ρ_{BRxz} for all the specimens after curing

The results show a trend of increasing in the bulk resistivity of the treated specimens especially in the *xx* direction when compared with the reference specimens. The bulk resistivity also shows correlation with the values of the curing electrical field, in which, increasing the curing electrical field increases the bulk resistivity. However, this correlation is more apparent when the measurements were taken immediately after the demolding of the specimens. This observation can be attributed to the water content of the specimens, where it was noted that the DC curing moves the water ions toward the anode which withdraw some of the water content of the specimen. This withdrawal of moisture is known in the literature as electroosmosis effect [25], and was noticed on all the DC-cured specimen. The amount of the withdrawn moisture increased when the curing electrical field increased. Some specimens were oven dried, then their bulk resistivity was measured. The bulk resistivity of the oven-dried specimens was very high, which highlights the known fact that the electrical conductivity of concrete depends on the moisture content [21]. The DC curing is responsible of polarizing the ions in the fresh cement pastes. This polarization seems to be permanent, which means that even after the specimens were dried and lost their electrical properties, the electrical behavior was

restored to some extent when the specimens were reintroduced to water. While increasing the curing electrical field increased the produced piezoelectric voltage [29], the bulk resistivity also increased. This behavior is expected in the testing arrangement that were used for this work shown in Figure 3. The mentioned arrangement represents a capacitor with an insulating material sandwiched by 2 opposite conductive plates. When the material insulating material of the capacitor (i.e cement paste specimen in this experiment) has the tendency of storing charged ions, the passing of the electrical current will be hindered until the charge is built up. The better piezoelectric performance of the treated specimens proved that significant permanent polarization occurred to them. Hence, the treated specimens have more capability to store the electrical charge, and as a result increase the bulk resistivity of the cement paste by hindering the testing current. The increase in the resistivity of the specimens due to polarization was discussed to some extent in the work of Cao and Chung [23].

Comparisons of the mean values of ρ_{BRxx}, based on the mixing water, of all the specimens at demolding and after the curing are shown in Figure 10, and Figure 11, respectively. The mentioned figures show the values in the *xx*-direction; however, it should be noted that all the other directions have the same behavior. The values of the bulk resistivity of the T water specimens are mostly greater than the DI water specimens both at demolding and after curing. This can be attributed to the better polarization of the specimens due to the larger amount of ions existed in the fresh cement paste. In addition, the difference between the connecting lines between the values of the T water and DI specimens is greater after curing when compared with the values at demolding. This observation suggests that the degree of hydration in the T water specimens was lesser than its DI counterparts. Since the electroosmotic water expulsion has greater effect on the T water specimens, it is expected to have more moisture gradient during hardening which retards the hydration process. During the water curing the hydration process continue and it is expected that the T water specimens will experience more hydration. The new hydration products will form inside the capillary pores of the cement paste which further reduce its radii, as well as, the capillary connectivity [32]. The described hydration effect is also apparent when comparing the bulk resistivity of the reference specimens at demolding and after curing. The bulk resistivity values of the reference specimens were very low when compared to the treated specimen at demolding. However, the values increased significantly and approached the values of the treated specimens after curing due to the resuming of the hydration process.

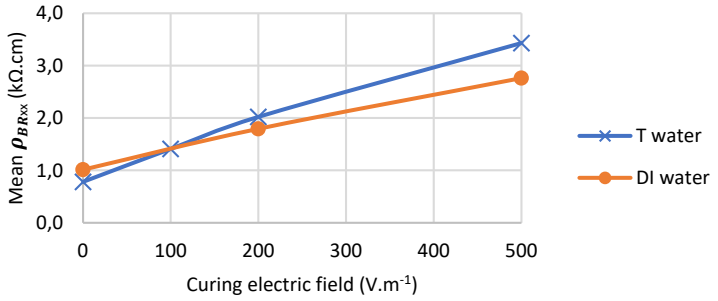

Figure 10: Comparison of the mean values of ρ_{BRxx} for all the specimens at demolding

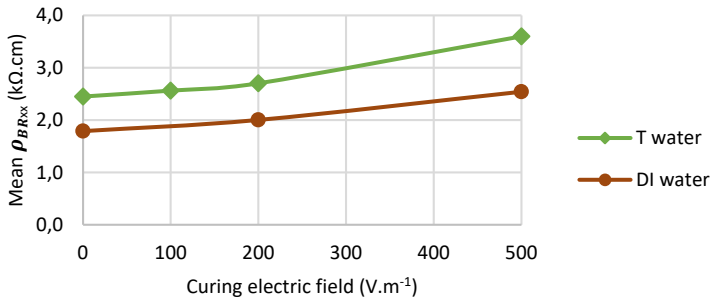

Figure 11: Comparison of the mean values of ρ_{BRxx} for all the specimens after curing

The results of the compression test of the T water specimens are shown in Figure 12. The results show that curing the cement paste under the effect of a DC has a significant effect on its mechanical properties. The ultimate compressive strength of the treated specimens was reduced by more than 50% when compared with the reference specimens. Moreover, the stress-strain diagram shows a significant decrease in the stiffness of the treated specimens, as well as, an increase of the rupture strain reaches 500%. While these results might limit the use of the DC curing process of cement hydrates in structural purposes, it is beneficial for the self-sensing purposes. Cement pastes that have more tolerance for large strains and lower modulus of elasticity can exhibit more elastic behavior, as well as, greater sensitivity to the applied loads. Hence, in a real-world reinforced concrete structures, the use of the cement hydrates that are treated with DC should be limited to sensing purposes. The zig-zag behavior, the lower ultimate compressive strength, and the higher strain values of the DC-treated specimens are all indication of internal damage of the microstructure of the cement paste. This can be attributed to the electroosmotic swelling of the pores

during the polarization process, which could cause micro-cracks to develop in the cement paste during the hardening process [25]. The higher density of the polarized specimens [29] suggest that it should exhibit better mechanical properties when compared with the reference specimens [33]. However, the testing shows contrary results, which can be attributed to the presence of a network of mico-cracks resulted from the electroosmosis effect on the tips of the pores inside the treated specimens [25]. Hence, further investigation on the hydration process of the cement paste that is cured under the effect of DC is needed to better understand the effect of such treatment on the mechanical properties of the cement paste. Another aspect that worth investigating, is the effect of the polarization time on the mechanical properties. Curing the fresh cement paste under the effect of DC for short periods of time immediately after casting might polarize the paste without damaging the internal structure of the hardened product.

The compressive strength test revealed an interesting inner morphology of the DC treated specimens as shown in Figure 13. The magnified piece in the figure shows a pattern of parallel curved lines that extend between the two electrodes, while the reference specimens did not show the same patterns. These patterns can be attributed to the electromigration of the C-S-H ions during the process of the DC curing. Since the application of the DC field continued while the hardening process of the cement paste take place, these patterns are permanent even after removing the DC field.

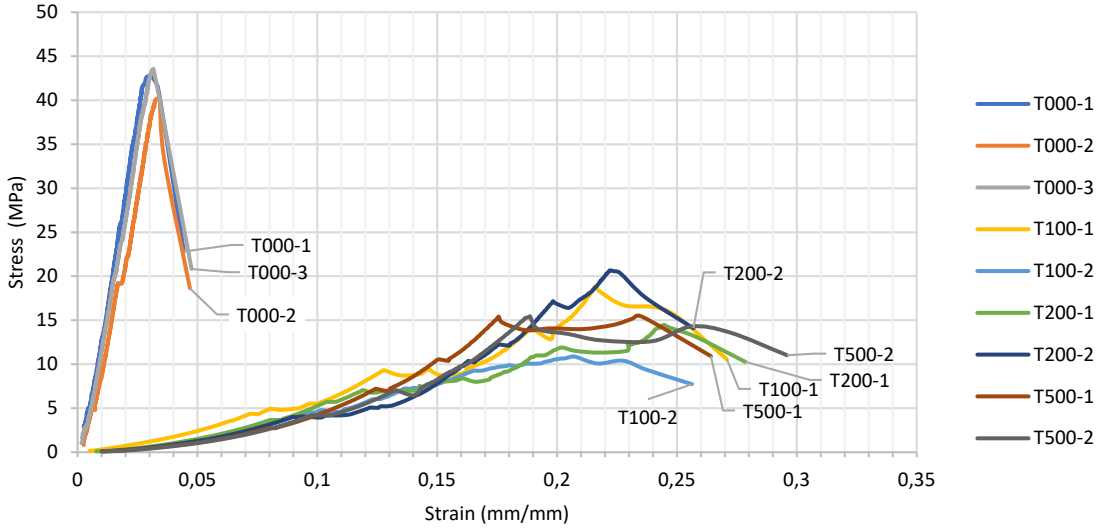

Figure 12: Stress-strain curves of the tested specimens

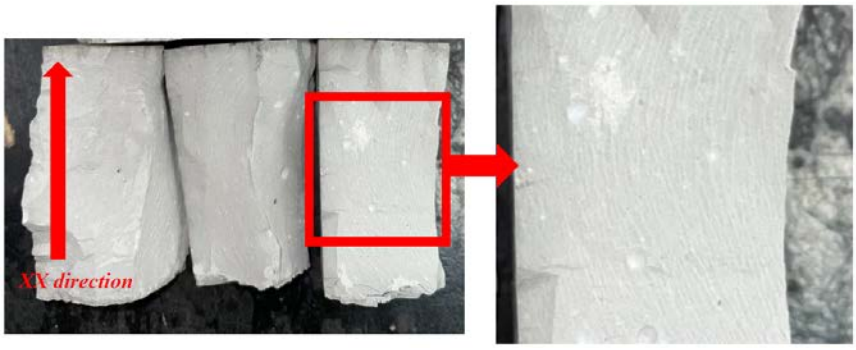

Figure 13: Typical morphology of the treated specimens

4 CONCLUSION AND FUTURE WORK

The DC curing of the fresh cement paste has a significant and permanent effect on the electrical and mechanical properties of the treated specimens. The following points were concluded from the results of the tested specimens:

- The bulk resistivity values of the treated specimens are higher than their reference counterparts. The higher the polarizing electrical field, the higher is the bulk resistivity of the hardened specimen.
- The bulk resistivity of the treated specimens increased in the direction of the polarization, as well as the other 2 perpendicular directions. This increase can be attributed to the increase in the capability of the polarized specimen to store the electrical charge, which hinders the passing of the testing current through the specimen.
- The strength and stiffness of the treated specimens were decreased, while the strain was increased when compared to the reference specimens. This behavior might be suitable for sensing purposes; however, it limits the use of this technique on cement hydrates that are intended for structural purposes.

The results demand more investigation on the mechanical properties of the DC-polarized specimens. In addition, studying the hydration process, and the morphology of the microstructures of the hydration products can contribute in better understanding of the mechanical behavior of the treated cement paste. More work is also required to study the effect of the time of application of the polarizing current on the mechanical behavior of the cement pastes.

5 ACKNOWLEDGMENT

The author would like to acknowledge the Deanship of the Scientific Research of Mutah University for funding this research as part of the Materials' Science and Energy Lab (MSEL) under the grant number (428/2021).

6 REFERENCES

[1] Mixajlovna, T. V., Nikolaevich, P. A., Yurievich, I. M., & Yurievich, A. V. (2020). Integral monitoring of high-rise buildings while minimizing the number of sensors. Journal of Applied Engineering Science, 18(4), 649–664. https://doi.org/10.5937/jaes0-29432

[2] Han, B., Wang, Y., Dong, S., Zhang, L., Ding, S., Yu, X., & Ou, J. (2015). Smart concretes and structures: A review. Journal of Intelligent Material Systems and Structures, 26(11), 1303–1345. https://doi.org/10.1177/1045389X15586452

[3] Chung, D. D. L. (2021). Self-sensing concrete: from resistance-based sensing to capacitance-based sensing. International Journal of Smart and Nano Materials, 12(1), 1–19. https://doi.org/10.1080/19475411.2020.1843560

[4] Buasiri, T., Habermehl-Cwirzen, K., & Cwirzen, A. (2019). State of the Art on Sensing Capability of Poorly or Nonconductive Matrixes with a Special Focus on Portland Cement–Based Materials. Journal of Materials in Civil Engineering, 31(11), 03119003. https://doi.org/10.1061/(asce)mt.1943-5533.0002901

[5] Rehman, S. K. U., Kumarova, S., Memon, S. A., Javed, M. F., & Jameel, M. (2020). A review of microscale, rheological, mechanical, thermoelectrical and piezoresistive properties of graphene based cement composite. Nanomaterials, 10(10), 1–42. https://doi.org/10.3390/nano10102076

[6] Al-Qaralleh, M., & Toutanji, H. (2018). Analytical Life-Prediction Model for RC Beams Strengthened with Externally Bonded FRP Laminates under Flexural Fatigue Loading. Journal of Composites for Construction, 22(6), 6018002. https://doi.org/10.1061/(ASCE)CC.1943-5614.0000892

[7] Bekzhanova, Z., Memon, S. A., & Kim, J. R. (2021). Self-sensing cementitious composites: Review and perspective. Nanomaterials, 11(9). https://doi.org/10.3390/nano11092355

[8] Whittington, H. W., McCarter, W. J., & Forde, M. C. (1981). The conduction of electricity through concrete. In Magazine of Concrete Research (Vol. 33, Issue 114, pp. 48–60). https://doi.org/10.1680/macr.1981.33.114.48

[9] Chen, P.-W., & Chung, D. D. L. (1993). Carbon fiber reinforced concrete for smart structures capable of non-destructive flaw detection. Smart Materials and Structures, 2(1), 22–30. https://doi.org/10.1088/0964-1726/2/1/004

[10] Sun, M., Liu, Q., Li, Z., & Hu, Y. (2000). A study of piezoelectric properties of carbon fiber reinforced concrete and plain cement paste during dynamic loading. 30, 1593–1595.

[11] Yeol, S., Viet, H., & Joo, D. (2019). Self-stress sensing smart concrete containing fine steel slag aggregates and steel fibers under high compressive stress. Construction and Building Materials, 220, 149–160. https://doi.org/10.1016/j.conbuildmat.2019.05.197

[12] Al-Bayati, A. J., Butrouna, K., Robert, S., Salman, B., & Al-Qaralleh, M. (2021). Utilizing Graphite Powder to Improve Concrete Conductivity, Compressive Strength, and Workability. In Construction Research Congress 2020 (pp. 881–888). https://doi.org/doi:10.1061/9780784482889.093

[13] Topu, I. B., Uygunolu, T., & Hocaolu, I. (2012). Electrical conductivity of setting cement paste with different mineral admixtures. Construction and Building Materials, 28(1), 414–420. https://doi.org/10.1016/j.conbuildmat.2011.08.068

[14] Schwarz, N., DuBois, M., & Neithalath, N. (2007). Electrical conductivity based characterization of plain and coarse glass powder modified cement pastes. Cement and Concrete Composites, 29(9), 656–666. https://doi.org/10.1016/j.cemconcomp.2007.05.005

[15] Tian, Z., Li, Y., Zheng, J., & Wang, S. (2019). A state-of-the-art on self-sensing concrete : Materials , fabrication and properties. Composites Part B, 177(May), 107437. https://doi.org/10.1016/j.compositesb.2019.107437

[16] Bastos, G., Patiño-Barbeito, F., Patiño-Cambeiro, F., & Armesto, J. (2016). Admixtures in cement-matrix composites for mechanical reinforcement, sustainability, and smart features. Materials, 9(12). https://doi.org/10.3390/ma9120972

[17] Han, B., Ding, S., & Yu, X. (2015). Intrinsic self-sensing concrete and structures : A review. MEASUREMENT, 59, 110–128. https://doi.org/10.1016/j.measurement.2014.09.048

[18] D'Alessandro, A., Rallini, M., Ubertini, F., Materazzi, A. L., & Kenny, J. M. (2016). Investigations on scalable fabrication procedures for self-sensing carbon nanotube cement-matrix composites for SHM applications. Cement and Concrete Composites, 65, 200–213. https://doi.org/10.1016/j.cemconcomp.2015.11.001

[19] Yoo, D.-Y., You, I., & Lee, S.-J. (2017). Electrical Properties of Cement-Based Composites with Carbon Nanotubes, Graphene, and Graphite Nanofibers. In Sensors (Vol. 17, Issue 5). https://doi.org/10.3390/s17051064

[20] Chung, D. D. L., & Wang, Y. (2018). Capacitance-based stress self-sensing in cement paste without requiring any admixture. Cement and Concrete Composites, 94(June), 255–263. https://doi.org/10.1016/j.cemconcomp.2018.09.017

[21] Shi, K., & Chung, D. D. L. (2018). Piezoelectricity-based self-sensing of compressive and flexural stress in cement-based materials without admixture requirement and without poling. Smart Materials and Structures, 27(10). https://doi.org/10.1088/1361-665X/aad87f

[22] Dong, B., Xing, F., & Li, Z. (2007). The study of poling behavior and modeling of cement-based piezoelectric ceramic composites. Materials Science and Engineering A, 456(1–2), 317–322. https://doi.org/10.1016/j.msea.2006.11.139

[23] Cao, J., & Chung, D. D. L. (2004). Electric polarization and depolarization in cement-based materials, studied by apparent electrical resistance measurement. Cement and Concrete Research, 34(3), 481–485. https://doi.org/10.1016/j.cemconres.2003.09.003

[24] Layssi H., Ghods, P., Alizadeh, Aali, R., & Salehi, M. (2016). Electrical Resistivity of Concrete. Concrete International, MAY 2015, 41–46.

[25] Sohn, D., & Mason, T. O. (1998). Electrically induced microstructural changes in portland cement pastes. Advanced Cement Based Materials, 7(3–4), 81–88. https://doi.org/10.1016/S1065-7355(97)00056-4

[26] ASTM C1202. (2012). Standard Test Method for Electrical Indication of Concrete's Ability to Resist Chloride Ion Penetration. American Society for Testing and Materials., C, 1–8. https://doi.org/10.1520/C1202-12.2

[27] Yuan, L., Li, J.-F., & Viehland, D. (1995). Electrically Induced Shape Changes in Hardened Cement Pastes and Porous Silica Gels: The Dynamic Nature of Gel Pore Structures during Water Transport. Journal of the American Ceramic Society, 78(12), 3233–3243. https://doi.org/https://doi.org/10.1111/j.1151-2916.1995.tb07959.x

[28] Al-Qaralleh, M. (2022). Self-Sensing Capabilities of Cement Pastes Treated by Direct Current Curing Technique. The 5th International Conference on Smart Materials Applications (ICSMA 2022).

[29] Al-Qaralleh, M. (2022). Piezoelectric behavior of polarized fresh cement pastes under the effect of different direct current voltages. Results in Engineering, 14(March), 100430. https://doi.org/10.1016/j.rineng.2022.100430

[30] Al-Qaralleh, M. (n.d.-ad). Effect of Water Cement Ratio on the Electrical Conductivity and Piezoelectricity of Cement Paste Cured While Applying Direct Current. Mutah for Resesrch and Studies: Natural and Applied Sciences. https://ejournal.mutah.edu.jo/index.php/NASS

[31] ASTM C109/C109M−20b. (2016). Standard test method for compressive strength of hydraulic cement mortars (Using 2-in . or [50-mm] cube specimens). Chemical Analysis, 04(C109/C109M – 11b), 1–9. https://doi.org/10.1520/C0109

[32] Sánchez, I., Nóvoa, X. R., de Vera, G., & Climent, M. A. (2008). Microstructural modifications in Portland cement concrete due to forced ionic migration tests. Study by impedance spectroscopy. Cement and Concrete Research, 38(7), 1015–1025. https://doi.org/10.1016/j.cemconres.2008.03.012

[33] Al-Lami, M. S. (2021). Correlation between permeability and porosity with other properties of concrete. Journal of Applied Engineering Science, 19(2), 538–546. https://doi.org/10.5937/jaes0-27267

Paper submitted: 29.09.2022.

Paper accepted: 12.12.2022.